Use of Viscogens, dNTPαS, and Rhodium(III) as Probes in Stopped-Flow Experiments To Obtain New Evidence for the Mechanism of Catalysis by DNA Polymerase β[†,‡]

Marina Bakhtina,[§] Soojin Lee,[§] Yu Wang,[§] Chris Dunlap,[§] Brandon Lamarche,[§] and Ming-Daw Tsai*[,§,||]

Departments of Chemistry and Biochemistry and Ohio State Biochemistry Program, The Ohio State University, Columbus, Ohio 43210, and Genomics Research Center, Academia Sinica, Taipei, Taiwan

Received November 2, 2004; Revised Manuscript Received January 3, 2005

ABSTRACT: The kinetic mechanism and the structural bases of the fidelity of DNA polymerases are still highly controversial. Here we report the use of three probes in the stopped-flow studies of Pol β to obtain new, direct evidence for our previous interpretations: (a) Increasing the viscosity of the reaction buffer by sucrose or glycerol is expected to slow down the conformational change differentially, and it was shown to slow down the first (fast) fluorescence transition selectively. (b) Use of dNTPαS in place of dNTP is expected to slow down the chemical step preferentially, and it was shown to slow down the second (slow) fluorescence transition selectively. (c) The substitution-inert Rh(III)dNTP was used to show for the first time that the slow fluorescence change occurs after mixing of Pol β·DNA·Rh(III)dNTP with Mg(II). These results, along with crystal structures, suggest that the subdomain-closing conformational change occurs *before* binding of the catalytic Mg(II) while the rate-limiting step occurs *after* binding of the catalytic Mg(II). These results provide new evidence to the mechanism we suggested previously, but do not support the results of three recent papers of computational studies. The results were further supported by a "sequential mixing" stopped-flow experiment that used no analogues, and thus ruled out the possibility that the discrepancy between experimental and computational results is due to the use of analogues. The methodologies can be used to examine other DNA polymerases to answer whether the properties of Pol β are exceptional or general.

The kinetic and structural basis of high-fidelity DNA replication by DNA polymerases has been a subject of extensive studies for several decades. As summarized in a review in 2000 (*2*), these studies led to the generally accepted view that the major controlling factor of fidelity is a rate-limiting conformational change that involves major movements of subdomains. However, on the basis of pre-steady-state kinetics and structural studies, we recently suggested that this may not be universally true and that the chemical step is likely to be the rate-limiting step and the main step contributing to the fidelity of some DNA polymerases, as discussed in ref *3*. Our results and recent results from other labs with different viewpoints for different DNA polymerases are summarized in a 2004 review (*4*). It is important to point out that a thorough understanding of the basis of DNA polymerase fidelity will require establishment of the complete kinetic mechanism, microscopic rate constants, and structural characterization of all intermediates, for both correct and incorrect dNTP[1] incorporations. Controversy in this field persists because such a complete picture has not yet been established for any polymerase, even for correct dNTP incorporation, let alone incorrect dNTP incorporation. Our laboratory has been working toward this goal using DNA polymerase β (Pol β) as a model system (*1*, *5*−*9*), as summarized below.

A series of crystal structures of binary and ternary complexes of Pol β indicates that, like most other DNA polymerases, Pol β undergoes an "open-to-closed" conformational change that is induced by dNTP binding (*10*−*13*). In 1997 we first applied stopped-flow fluorescence assays to monitor conformational changes associated with the catalytic cycle of Pol β. The observed biphasic change in fluorescence was initially interpreted to represent multiple conformational changes accruing before the phosphodiester bond formation step (chemistry step) (*6*), in accordance with the widely accepted concept of a rate-limiting conformational change at that time. Later, using Cr(III)dNTP exchange-inert complexes we showed that the crystal structure of the E·DNA·Cr(III)dNTP ternary complex (in the absence of catalytic metal ion) already exists in the closed form (*6*). These results, along with the observation that Cr(III)dNTP

† This work was supported by NIH Grant GM43268.

‡ This is paper 11 in the series "DNA Polymerase β". For paper 10, see ref *1*.

* Author to whom correspondence should be addressed, at the Department of Chemistry. Tel: (614) 292-3080. Fax: (614) 292-1532. E-mail: tsai.7@osu.edu.

§ The Ohio State University.

|| Genomics Research Center, Academia Sinica.

[1] Abbrevations: Pol β, *Rattus norvegicus* DNA polymerase beta; dNTP, 2′-deoxynucleoside 5′-triphosphate; dCTPαS, 2′-deoxycytidine 5′-*O*-(1-thiotriphosphate); M·dNTP, metal ion 2′-deoxynucleoside 5′-triphosphate complex; Rh(III)dCTP, rhodium(III) 2′-deoxycytidine 5′-triphosphate; 2-AP, 2′-deoxy 2-aminopurine; MOPS, 3-(*N*-morpholino)-propanesulfonic acid; BTP, 1,3-bis[tris(hydroxymethyl)methylamino]-propane; DTT, dithiothreitol.

10.1021/bi047664w CCC: $30.25
Published on Web 03/10/2005

Scheme 1: Kinetic Scheme of Single-Nucleotide Incorporation[a]

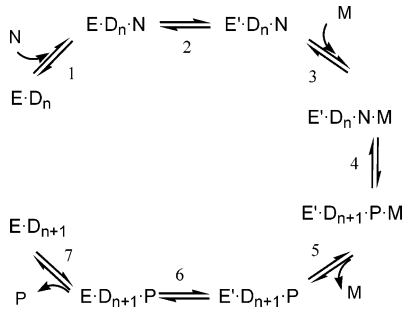

[a] Reproduced with changes from ref *6*. E = Pol β in open finger conformation; E′ = Pol β in closed finger conformation; D_n = DNA; N = M·dNTP; M = catalytic metal ion; P = M·PP_i. In the text, the *binary* complex refers to the E·D_n state, while the *ternary* complex refers to the E′·D_n·N state (after the conformational change).

can induce only the faster phase of fluorescence transition in the absence of the catalytic metal ion (*8*), led us to conclude that the subdomain-closing conformational change of Pol β is already complete before the step giving rise to the slow phase of fluorescence transition. This conclusion has also been supported by other reports (*14*−*16*). The stopped-flow transient fluorescence results have been further substantiated under a variety of conditions (*1*), and the rate of the slow phase has been shown to be identical to the rate of dNTP incorporation. A simplified kinetic scheme has been proposed as shown in Scheme 1, which involves a fast subdomain-closing conformational change, E to E′, induced by binding of M·dNTP, and a slow, rate-limiting chemical step (*6*).

While the above results represent significant advancement in the field, they also lead to new questions and new proposals. One is whether Pol β is an exception, as has been raised by us (*3*) and others (*4*, *15*, *17*, *18*). This question remains to be addressed by applying our and other experimental approaches to other polymerases. In this paper we address only the following issues related to Pol β. (a) Even though we have suggested that the rates of the fast and the slow fluorescence transitions (see Figure 1 in the Results section) correspond to the rates of the subdomain-closing conformational change and the chemical step, respectively (*6*), there has been no direct evidence linking the fluorescence transitions with the specific steps. Thus strictly we can only state that the subdomain closing conformational change is a fast step, and that the slow phase more likely represents a step limited by chemistry (*1*, *3*). (b) It has been proposed on the basis of dynamic simulation studies that a subtle conformational change preceding chemistry, involving Arg258 rotation induced by binding of the catalytic magnesium ion, is fluorescence silent but is the rate-limiting step in the Pol β catalytic cycle (*19*, *20*). (c) Recent computational studies suggest that Pol β subdomain closing requires the presence of both nucleotide-binding and catalytic metal ions. Since the crystal structure of the E·DNA·Cr(III)dNTP ternary complex exists in the closed form, the authors rationalized their contradictory finding by invoking differences between Cr(III) and Mg(II) (*21*).

In this paper we report the combined use of viscogens (sucrose and glycerol), dNTPαS, and rhodium(III) as mechanistic probes to further address the issues mentioned above.

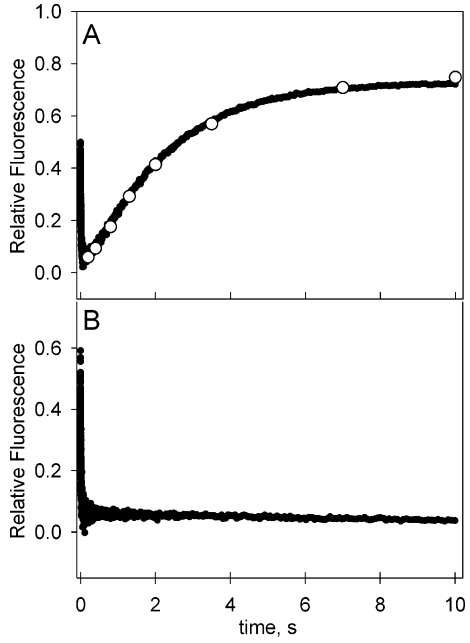

FIGURE 1: (A) Superimposition of stopped-flow tryptophan fluorescence (●) and rapid chemical quench (○) assays for incorporation of dCTP into the 18/36AP DNA substrate. The reaction was initiated by rapid mixing of solutions from two syringes: the first syringe contained 600 nM 18/36AP with 900 nM Pol β; the other syringe contained 200 μM dCTP and 10 mM $MgCl_2$. The rapid quench data points fit to a single exponential (eq 1) with a rate constant of 0.430 s^{-1}. The stopped-flow data points fit to a double exponential (eq 3) with k_1 = 64.4 s^{-1} and k_2 = 0.457 s^{-1}. (B) Stopped-flow tryptophan fluorescence assays with dideoxy-terminated DNA substrate. One syringe contained Pol β and 18dd/36AP DNA substrate. The other syringe contained dCTP and $MgCl_2$. The data points fit to the single exponential (eq 2), with a rate constant of 69.9 s^{-1}.

Two of the three probes, buffer viscosity and Rh(III)dNTP, have not previously been used in stopped-flow studies of DNA polymerases, and dNTPαS has been used only rarely. Application of viscogens and dNTPαS led to new direct evidence that the rates of the fast and slow fluorescence transitions correspond to the rates of the conformational change and the chemical steps, respectively. The results of experiments with Rh(III)dNTP allowed dissection of the nucleotide-bound metal ion and the catalytic metal ion, and provide direct evidence that the rate-limiting step occurs *after* binding of Mg(II) to the polymerase·DNA·MdNTP ternary complex. The possibility of the use of analogues (metal ions or dideoxy-terminated primers) as the reason for the discrepancy of our experimental results with the results of computational studies was further addressed by sequential stopped-flow experiments without using any analogue.

MATERIALS AND METHODS

Materials. Ultrapure dNTP's and G-25 Microspin columns were purchased from Amersham Biosciences. Sp-dCTPαS (>95% pure) was purchased from Biolog-Life Science Institute. Radiolabeled [γ-^{32}P]ATP was purchased from MP Biomedicals. T4 polynucleotide kinase was obtained from New England BioLabs. Reverse phase C_{18} cartridges were obtained from the Waters Corp. All other chemicals used were obtained from Sigma-Aldrich.

DNA Polymerase β Purification. Recombinant rat Pol β was purified as previously described from an overexpressing

Scheme 2: Sequences of DNA Substrates[a]

18/36AP

5'- GCC TCG CAG CCG TCC AAC
3'- CGG AGC GTC GGC AGG TTG GT**Ã** TCA GTG GAG TTA GGT

18dd/36AP

5'- GCC TCG CAG CCG TCC AA**C**$_{dd}$

3'- CGG AGC GTC GGC AGG TTG GT**Ã** TCA GTG GAG TTA GGT

19/36AP

5'- GCC TCG CAG CCG TCC AAC C
3'- CGG AGC GTC GGC AGG TTG GT**Ã** TCA GTG GAG TTA GGT

19dd/36AP

5'- GCC TCG CAG CCG TCC AAC **C**$_{dd}$
3'- CGG AGC GTC GGC AGG TTG GT**Ã** TCA GTG GAG TTA GGT

18/35AP

5'- GCC TCG CAG CCG TCC AAC
3'- CGG AGC GTC GGC AGG TTG G**Ã**T CAG TGG AGT TAG GT

18dd/35AP

5'- GCC TCG CAG CCG TCC AA**C**$_{dd}$
3'- CGG AGC GTC GGC AGG TTG G**Ã**T CAG TGG AGT TAG GT

[a] **Ã** represents 2-aminopurine; $\mathbf{C}_{dd}$ represents 2′,3′-dideoxycytidine 5′-monophosphate.

Escherichia coli strain BL21(DE3)(pLysS, pET17-Pol β) (*22*). The Pol β concentration was determined by UV absorbance at 280 nm using extinction coefficient of 21200 M^{-1} cm^{-1}. The enzyme appeared to be homogeneous on the basis of SDS/PAGE developed using the silver staining method.

DNA Substrates. The sequences of primer/template DNA substrates used in this study are shown in Scheme 2. Custom synthesized oligomers were purchased from Integrated DNA Technologies (Coralville, IA). Each DNA oligomer was further purified by 18% (w/v) polyacrylamide/7 M urea denaturing gels and extracted with 500 mM ammonium acetate and 1 mM EDTA. Extracted oligomers were subsequently desalted on a Sep-Pak C_{18} cartridge and eluted using methanol:water (60:40). After removing the solvent with vacuum, the oligomers were resuspended in TE buffer (10 mM TrisHCl, 0.1 mM EDTA, pH 8.0) and the concentration was determined by UV using a calculated molar absorption coefficient (*23*). The oligomers were then stored at −20 °C.

DNA substrates used in the chemical quench experiments were 5′-end labeled using T4 polynucleotide kinase and [γ-^{32}P]ATP (4500 Ci/mol) according to the manufacturer's protocol. The T4 polynucleotide kinase was inactivated by heating at 65 °C for 20 min. The labeled 18-mer primer was separated from unreacted ATP and Mg(II) using a G-25 microspin column with a small amount of Chelex 100 resin added to it. The appropriate unlabeled DNA-template was added and allowed to anneal by heating to 80 °C followed by gradual cooling to room temperature.

Synthesis of Rh(III)dNTP Phosphate Complex and Precomplex. Previously, Rh(III)ATP was synthesized and well characterized (*24*). In this complex Rh(III) coordinates with the phosphate moiety and is called the "phosphate complex" in this paper, to be differentiated from the newly identified "precomplex". The same procedure was followed to synthesize the Rh(III)dCTP phosphate complex. Briefly, 10 mM $Rh(H_2O)_6^{3+}$ (with ClO_4^- as counterions) was reacted with 10 mM dCTP at pH 3.0 and 80 °C for 20 min. $Rh(H_2O)_6(ClO_4)_3$ was prepared from rhodium(III) chloride hydrate as described by Ayres and Forrester (*25*). Product formation was monitored by ^{31}P NMR. The product was purified by running sequentially through Dowex-1 ion exchange and G-10 gel filtration columns. The product was shown to consist of a mixture of bidentate and tridentate isomers showing ^{31}P NMR properties similar to those described for Rh(III)ATP (*24*). Additional characterization was performed by ^{1}H NMR and ^{13}C NMR. The ^{13}C NMR spectrum of Rh(III)dCTP was very similar to that of free dCTP, which ruled out the possibility of a deaminated product.

The precomplex of Rh(III)dCTP was synthesized by heating 10 mM Rh(III) chloride hydrate with 10 mM dCTP at pH 3.0 and 80 °C for 20 min. Product formation was monitored by ^{1}H NMR and ^{31}P NMR, which indicated that the Rh(III) ion coordinates with the cytosine ring but not with the phosphate. Further studies suggested that it is likely an intermediate for the formation of the phosphate complex and it was thus designated as the "precomplex". The extensive details are described in the Supporting Information.

Kinetic Assays. The standard assay buffer consisted of 100 mM MOPS, 50 mM KCl, 10% (v/v) glycerol, 1 mM DTT at pH 7.0; and the typical assay was conducted at 25 °C. The viscosity-dependence study was performed with varying concentrations of either sucrose or glycerol. Stopped-flow experiments with the dNTPαS substrate analogue were performed at 37 °C in a buffer consisting of 100 mM BTP, 50 mM KCl, 10% (v/v) glycerol, and 1 mM DTT at pH 6.8.

Chemical Quench Experiments. A rapid quench instrument (KinTek instrument Corp, State College, PA) was used for reaction times ranging from 5 ms to 100 s. Pol β and DNA were preincubated for at least for 5 min before the start of the reaction. The typical reaction mixture consisted of 100 nM DNA, 300 nM Pol β, 100 μM dCTP, and 5 mM $MgCl_2$ (all final concentrations) in the standard assay buffer described above. Reaction was rapidly quenched by mixing with EDTA (300 mM, final concentration). Reaction products were then mixed 1:1 with formamide and run on an 18% (w/v) polyacrylamide/7 M urea denaturing gel. The disappearance of substrate and the formation of product were analyzed with a STORM 840 PhosphorImager (Molecular Dynamics).

Stopped-Flow Fluorescence Assays. Experiments were performed on an Applied Photophysics SX 18MV stopped-flow apparatus. The excitation wavelengths were 285 and 312 nm for tryptophan and 2-aminopurine, respectively, with a spectral bandpass of 4 nm. Emission was monitored using a 340 nm bandpass filter (Corion, 10 nm) for tryptophan and a 360 nm high pass filter (Corion) for 2-aminopurine. All buffers were filtered with a 0.45 μm filter and degassed prior to use. Primer and template oligomers were mixed at a 1.3:1 ratio and allowed to anneal by heating to 80 °C and then slow cooling to room temperature. Unless otherwise specified, the experiment involved rapid mixing of two solutions (80 μL each) in the standard assay buffer: (a) 600 nM annealed DNA substrate and 900 nM Pol β, and (b) 200 μM dCTP and 10 mM $MgCl_2$ (or 200 μM Rh(III)dCTP in

the absence of Mg(II)). Typically, a minimum of 10 runs were performed and averaged. Profiles were typically collected using a logarithmic time scale (10 s) with 1000 data points.

Data Analysis. Data obtained from rapid quench kinetic assays were fitted by nonlinear regression using Sigma Plot software (Jandel Scientific) with eq 1:

$$\% \text{ turnover} = A[1 - \exp(-kt)] \quad (1)$$

where A and k represent the amplitude and the observable rate constants, respectively. % turnover is defined by the ratio (product formed)/(substrate remained + product formed).

Stopped-flow data were fitted using Applied Photophysics software. Equations 2 and 3 were used where appropriate:

$$\text{signal} = A[1 - \exp(-kt)] + C \quad (2)$$

$$\text{signal} = A_1[1 - \exp(-k_1 t)] + A_2[1 - \exp(-k_2 t)] + C \quad (3)$$

where A is the amplitude, k is observable rate constant, and C is an offset constant.

RESULTS

DNA Substrates and Assay Conditions. (a) pH. Since Rh(III)dNTP complexes are unstable above pH 7.0 (*24*), the pH used in this study was 6.8−7.0. Our past work with Cr(III)dNTP was also performed at pH 6.8 for the same reason, while most other Pol β kinetic analyses have been performed in the pH range 7.6−8.0. *(b) Fluorophores.* It was shown in our previous work that the amplitude and direction of the fluorescence changes during the course of single nucleotide incorporation depends on the excited fluorophore, the DNA substrate, and the reaction conditions (*1*). This study used two fluorophore probes—Trp325 (the single tryptophan of Pol β) and 2-aminopurine—to monitor fluorescence changes associated with different enzyme−DNA conformations during the reaction pathway. *(c) DNA Substrates.* This study used three DNA substrates, 18/36AP, 19/36AP and 18/35AP, along with their dideoxy-terminated analogues, as shown in Scheme 2. For tryptophan fluorescence, it was found that the 18/36AP DNA substrate provides a good signal-to-noise ratio. As it has been shown previously, the best signal-to-noise ratio in the 2-aminopurine fluorescence stopped-flow experiments can be obtained with 2-AP modification in +1 position relative to the nascent base pair (*1*). Therefore 19/36AP and 18/35AP DNA substrates (Scheme 2) were chosen for presented studies.

Figure 1A shows the tryptophan fluorescence change for the incorporation of dCTP into DNA substrate 18/36AP. The observed biphasic curve fits well to a double exponential with $k_1 = 64.4$ s^{-1} and $k_2 = 0.457$ s^{-1}. The second rate is in good agreement with the rate of single nucleotide incorporation, obtained in the rapid quench experiment (0.430 s^{-1}, Figure 1A). This suggests that the rate of the slow phase of the fluorescence change and the rate of phosphodiester bond formation are determined by the same step in the reaction pathway. The "slow phase" is absent when using the dideoxy-terminated DNA substrate (Figure 1B). These results resemble previously published data (*1*) with the exception that in the present experiments the observed "slow phase" rate constant was smaller (0.457 s^{-1} vs 12.2 s^{-1}) due to the lower temperature (25 °C vs 37 °C) and lower pH (7.0 vs 8.0).

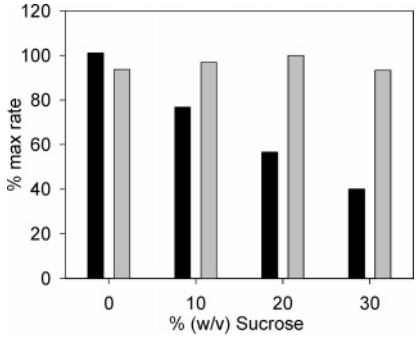

FIGURE 2: Effects of reaction buffer viscosity in stopped-flow fluorescence assay. Bars show % change of fast fluorescence transition (black) and slow fluorescence transition (gray) vs % (w/v) sucrose in the reaction buffer. For each reaction, one syringe contained Pol β with 18/35AP DNA substrate and 10 mM $MgCl_2$ in assay buffer with varying concentration of sucrose at 25 °C. The other syringe contained 200 μM dCTP and 10 mM $MgCl_2$ in the same sucrose containing assay buffer. 2-Aminopurine fluorescence was monitored during the reaction course, and the data were fit to a double exponential equation to obtain k_{obs1} (fast phase) and k_{obs2} (slow phase) as presented in Table 1.

Table 1: Effect of Reaction Buffer Viscosity on the Rates of the Fast and Slow Phases of Fluorescence Change in Stopped-Flow Assays[a]

	k_{obs1}, s^{-1} fast phase	k_{obs2}, s^{-1} slow phase
no viscogen	82.3	0.80
10% sucrose	62.5	0.83
20% sucrose	46.1	0.86
30% sucrose	32.6	0.80
10% glycerol	63.4	0.85
15% glycerol	57.8	0.85
20% glycerol	43.9	0.89
25% glycerol	41.0	0.90
30% glycerol	36.2	1.01
35% glycerol	30.4	1.04

[a] The % (w/v) viscogen is defined on the basis of 1 g of viscogen in 1 mL of buffer being 100%.

Increased Viscosity Differentially Slows the Fast Fluorescence Phase. Solvent viscosity as a probe of steps involving enzyme conformational changes has been successfully used before in steady-state experiments (*26*−*30*). If an enzyme reaction pathway includes a step involving spatial movements of segments of the enzyme, then by using an assay buffer with higher viscosity this step can be selectively perturbed (*27*, *31*). Here we report the application of viscogens in *pre-steady-state* stopped-flow studies of Pol β.

We first used sucrose, a common viscogen, to probe the observed biphasic fluorescence change in stopped-flow experiments. As can be seen in Figure 2 and Table 1, the rate of the fast fluorescence transition decreased significantly with increasing sucrose concentration in the reaction buffer, while the rate of the slow transition remained little changed. In order to make sure that the observed sucrose effect is caused by the increased buffer viscosity rather than by an interaction with sucrose, we performed analogous stopped-flow experiments with varied concentration of another viscogen, glycerol. As can be seen in Table 1, glycerol has similar effects on the rates of the fast fluorescence transition.

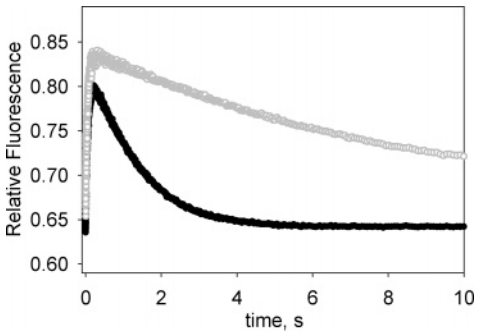

FIGURE 3: Effects of dCTPαS in 2-aminopurine fluorescence stopped-flow assay. One syringe contained 800 nM Pol β with 600 nM 18/36AP DNA substrate. The other syringe contained 1 mM dCTP (black ●) or dCTPαS (gray ○). The assay was conducted at 37 °C in an assay buffer consisting of 100 mM BTP, 10 mM $MgCl_2$, 50 mM KCl, 10% (v/v) glycerol, 1 mM DTT, pH 6.8. The reaction was initiated by mixing 80 μL solutions from each syringe, and 2-aminopurine fluorescence was monitored during the reaction course. The fluorescence change fits well to a double exponential (eq 3), with rate constants $k_1 = 13.9\ s^{-1}$ and $k_2 = 0.720\ s^{-1}$ for dCTP and $k_1 = 16.3\ s^{-1}$ and $k_2 = 0.103\ s^{-1}$ for dCTPαS.

Table 2: Thio Effects for the Fast and Slow Phases of Fluorescence Change in Stopped-Flow Assays

	k_{obs1}, s^{-1} fast phase	k_{obs2}, s^{-1} slow phase
dCTP	13.9	0.720
dCTPαS	16.3	0.103
thio effect, dCTP/dCTPαS	0.85	7.0

These results support that the fast fluorescence transition corresponds to a conformational change step and that this step involves considerable physical movement within the Pol β·DNA complex. This provides new evidence to our previous suggestion that the fast fluorescent transition corresponds to the subdomain-closing conformational change. The previous suggestion was based on the observation that the Pol β·DNA·Cr(III)dNTP complex already exists in the closed form (*6*); therefore the fluorescence change preceding this form was assigned to the subdomain-closing conformational change (*8*). The current evidence links the fast fluorescence change to a major conformational change, most likely the subdomain-closing step.

On the other hand, since the slow phase of the fluorescence change was not sensitive to viscosity, it more likely reflects the rate of the chemistry step, as further corroborated by the results in the next section.

dNTPαS Differentially Slows Down the Slow Fluorescence Phase. The dNTPαS substrate analogues have been used extensively in polymerase studies as a mechanistic probe of the chemical step (*7*, *17*, *32*−*36*), but this probe has rarely been used with the stopped-flow technique (*9*, *37*). Since it is generally accepted that this substrate analogue will perturb mainly the chemical step rather than the conformational step, we used dCTPαS to explore the thio effect in fluorescence transitions in the stopped-flow assay. The results in Figure 3 and Table 2 show that, while the rate of the fast phase is similar for both the natural substrate and its thio analogue, the rate of the slow fluorescence transition was significantly slower in the reaction with dNTPαS. These results agree with the data reported in our 1997 paper (*9*), except that the magnitudes of thio effect differ (4.3 in previous study and 7.0 in this study for the slow phase), due to different conditions used in the two studies (different pH and the use of pure Sp isomer in the present study). As mentioned in the introduction, we interpreted the two phases of fluorescence incorrectly at that time. The data obtained in this work support our new interpretation that the second (slow) fluorescence transition reflects the rate of the chemistry step since the slow phase is perturbed differentially by dNTPαS.

It is important to point out that the slow fluorescence transition is not likely caused by the phosphodiester bond formation directly. This is made evident by the fact that this transition is observed in both 2-aminopurine and tryptophan fluorescence assays, and that the tryptophan residue (Trp325) of Pol β is remote from the site of the chemical reaction. Instead, the fluorescence change is probably caused by another conformational change occurring after chemistry. Our working hypothesis is that the second fluorescence transition is due to the "subdomain reopening" (E′ to E, step 6 in Scheme 1), but its detection is limited by the rate of chemistry step. This point will be further addressed in the Discussion.

Properties of Rh(III)dCTP as an Analogue of Mg(II)dCTP in Pol β Catalysis. DNA polymerase structures suggest a two-metal ion mechanism for dNTP incorporation (*38*, *39*). These two Mg(II) ions are designated as the nucleotide-binding Mg(II) ion (as part of MgdNTP) and the catalytic Mg(II) ion. In 1998 we first used Cr(III)dTTP in a stopped-flow fluorescence assay to substitute for Mg(II)dTTP, allowing us to show that the fast phase of the fluorescence change is induced by metal·dNTP binding in the absence of the catalytic metal ion (*8*). The goal of the present work is to take this previous study one step further and to perform kinetic analyses starting from the Pol β·DNA·MdNTP (E′·D_n·N in Scheme 1) ternary complex. Since we were unable to accomplish this with Cr(III)dNTP, possibly because Cr(III)dNTP is not stable enough, we pursued the use of Rh(III)dNTP.

Unlike Mg(II)·nucleotide complexes, which are in rapid equilibrium in aqueous solution (with exchange rates of 5000 s^{-1} (*40*)), exchange-inert nucleotide complexes have ligand exchange rates measured in days, under nonbasic conditions (*41*). Exchange-inert metal·nucleotide complexes have been reported for Cr(III), Co(III) (*41*), and Rh(III) (*24*). Of these, Rh(III) has been used least frequently in enzymatic studies (*24*, *42*−*45*), and has never been used to study polymerases. Of the three metal nucleotide complexes studied, Rh(III)-NTP has been shown to be structurally most similar to Mg-(II)NTP. For example, the Rh- -O bond lengths are very similar to Mg- -O bond lengths (2.02 and 2.08 Å, respectively), as determined by X-ray structures with pyrophosphate (*46*, *47*).

In using substitution-inert complexes, it is important to keep in mind that their "inertness", or stability, differs from one another and is also very sensitive to a number of factors including pH and the other ligands at the coordination sphere. Furthermore, each complex, when formed, consists of a mixture of >10 positional isomers and stereoisomers (*41*). For the more stable complexes each isomer can be isolated and tested for enzymatic activity. This is how the inert complexes have been used conventionally. Though not usually specified, the noninert complex Mg(II)dNTP consists of a similar set of isomers (but with different distributions).

When Mg(II)dNTP binds to the enzyme, the enzyme is likely to accept more than one isomer (or even all isomers) at the ground state (step 1 in Scheme 1), but only one specific isomer can exist at the transition state. On the basis of our early study with adenylate kinase (*48*), we believe that in the process from ground state to transition state the enzyme is able to convert the incorrect isomer to the correct isomer for noninert complexes.

Our recent study with Pol β·Cr(III)dNTP and the present work with Rh(III)dNTP take advantage of these complicated and subtle properties described above. In the work with Cr(III)dNTP a mixture of stereoisomers was used directly. It was assumed that stereochemically incorrect isomers were converted to the correct stereoisomer in the process of catalysis, though it cannot be ruled out that some of the isomers were excluded from binding or released after binding (and it makes no difference to our result as long as all processes are fast). One single isomer was observed in the crystal structure of the intermediate (*6*). When Rh(III)dNTP (also as a mixture of isomers) was used for rapid quench experiments, the rate of incorporation was slower by a factor of 7 than when Mg(II)dCTP was used. While this could suggest that Rh(III) is not a good analogue of Mg(II), it could also be because Rh(III)dNTP isomers are more inert and the interconversion of different isomers becomes rate-limiting. This problem was overcome by using a "precomplex" of Rh(III)dCTP, which is a possible intermediate of the Rh(III)dCTP complex. As described in the Supporting Information, in the precomplex Rh(III) coordinates with the cytosine ring possibly through a nitrogen ligand, but not with the phosphates. This is not unreasonable, as Rh(III) has been shown to coordinate with the adenine ring but not the phosphate of AMP (phosphate in the outersphere) (*49*). For clarity, the Rh(III)dCTP complex with phosphate coordination was termed the "phosphate complex". All of the studies reported here used the precomplex, and the results indicate that it is a good analogue of the Mg(II)dCTP complex. We believe and hypothesize that the precomplex is more labile than the phosphate complex and that it is converted rapidly to the correct isomer of the phosphate complex after binding to the active site of Pol β.

Use of Rh(III)dCTP To Dissect Roles of Two Metal Ions. In this section, we describe reproduction of Cr(III)dNTP results using the Rh(III)dCTP precomplex. In addition, the conditions used in the previous Cr(III)dNTP studies allowed us to monitor only the reaction when the incoming nucleotide formed a non-natural pair with 2-aminopurine. Use of optimized stopped-flow assay conditions (*1*) allowed us to study the incorporation of the correct nucleotide to form the natural base pair C:G.

First, the Trp fluorescence was utilized to monitor changes in enzyme conformation during the reaction pathway. Figure 4A shows the Trp fluorescence change upon mixing preformed Pol β·DNA complex with Rh(III)dCTP complex in the absence of Mg(II). The observed fluorescence change fits well to single-exponential equation with $k_{obs} = 75.3\ s^{-1}$. In order to rule out the possibility that the observed fluorescence decay was a result of fluorescence quenching by $RhCl_3$ or dCTP, we performed a series of control stopped-flow experiments. The results indicated that neither dCTP nor $RhCl_3$ alone could induce noticeable fluorescence changes (Figure 4B,C).

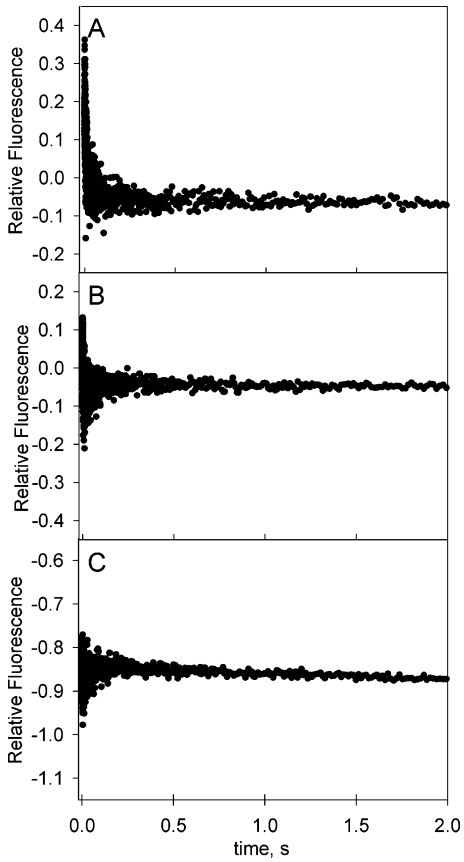

FIGURE 4: Rh(III)dCTP stopped-flow tryptophan fluorescence assays. (A) Syringe 1 contained Pol β with 18/36AP DNA substrate in assay buffer at 25 °C. Syringe 2 contained 200 μM Rh(III)-dCTP in assay buffer. The fluorescence change fits well to a single exponential (eq 2), with a rate constant of 75.3 s^{-1}. (B) Negative control for 1 mM dCTP alone in assay buffer in syringe 2, in the absence of Rh(III). (C) Negative control for 1 mM Rh(III) chloride hydrate alone in assay buffer in the absence of dCTP.

Second, 2-aminopurine fluorescence was used to monitor change in the enzyme·DNA conformation. Figure 5A shows the fluorescence change associated with incorporation of dCTP to 18/35AP by Pol β. Again, the fluorescence change has biphasic character; and the "slow phase" was abolished when chemistry was precluded by using dideoxy-terminated primer (not shown). As can be seen in Figure 5B, use of Rh(III)dCTP in the absence of Mg(II) resulted in the fast phase of fluorescence change only.

These results have reconfirmed the results we previously obtained with Cr(III)dNTP in that metal·dNTP alone (in the absence of the second catalytic metal ion) can induce the subdomain-closing conformational change. Furthermore, the use of Rh(III)dNTP analogues and optimized conditions allowed us to examine the reaction starting with the Pol β·DNA·Rh(III)dNTP ternary complex (the original goal of pursuing the use of rhodium in place of chromium ions), which led to new information as described in the next section.

Use of Rh(III)dCTP To Show That the Slow Step Occurs after Addition of Catalytic Mg(II). We next used stopped-flow experiments to directly observe the fluorescence change induced by binding of the second Mg(II) ion to the ternary complex. When Pol β was preincubated with DNA substrate and Rh(III)dCTP and the reaction was initiated by Mg(II), the "faster phase" of tryptophan fluorescence disappeared, and only the slow phase was observed (Figure 6A). The

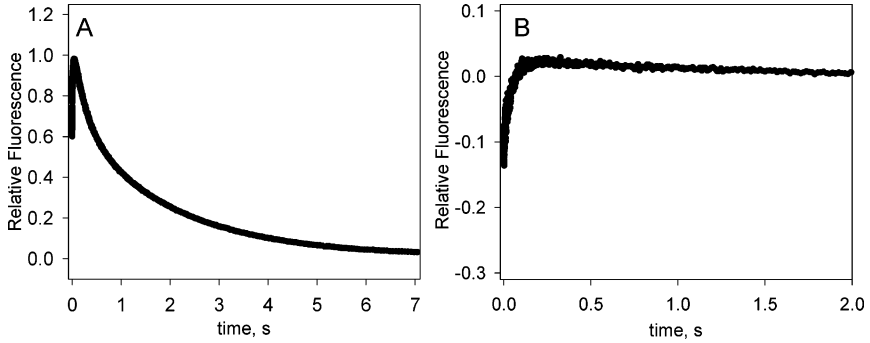

FIGURE 5: Stopped-flow 2-aminopurine fluorescence assays. (A) One syringe contained Pol β with 18/35AP DNA substrate in assay buffer at 25 °C. The other syringe contained 200 μM dCTP and 10 mM $MgCl_2$ in assay buffer. The fluorescence change has biphasic character with distinct fast and slow phases. (B) One syringe contained Pol β with 18/35AP DNA substrate in assay buffer at 25 °C. The other syringe contained Rh(III)dCTP in assay buffer. The slow fluorescence transition disappeared.

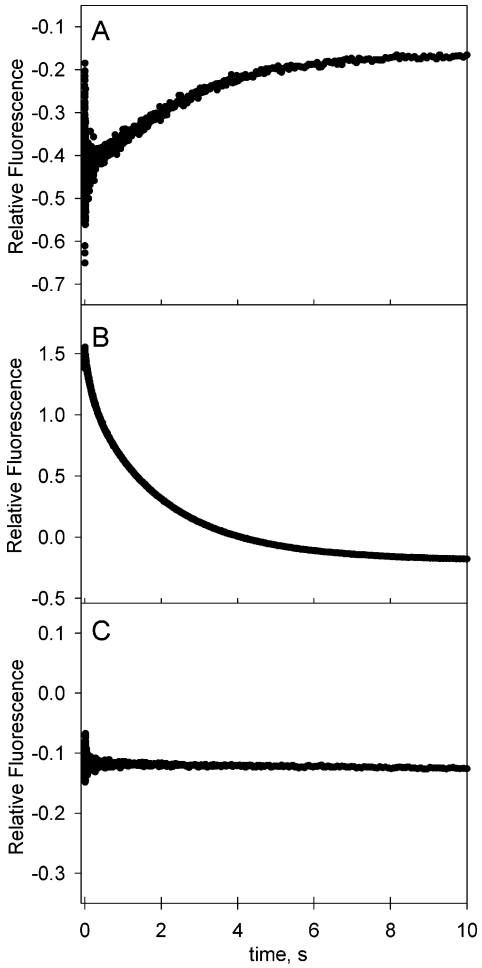

FIGURE 6: Stopped-flow fluorescence assays starting with the E·DNA·Rh(III)dNTP ternary complex. The reaction conditions for panels A and B are the same as those for Figure 4A and Figure 5B, respectively, except that Rh(III)dCTP is now included in syringe 1 instead of syringe 2, and 10 mM $MgCl_2$ is included in syringe 2. Panel C is a repetition of panel A with the dideoxy-terminated primer.

fluorescence transition has single-exponential character with the absence of any noticeable lag-phase. Similar results were also obtained in stopped-flow experiments by monitoring the change in 2-aminopurine fluorescence during the course of dCTP incorporation from ternary complex Pol β·18/35AP·Rh(III)dCTP (Figure 6B). The results in Figure 6 unequivocally demonstrate that the slow fluorescence change, which has the same rate as that of dNTP incorporation (as shown in Figure 1), occurs *upon addition of Mg*(*II*) to the enzyme·DNA·MdNTP ternary complex (step 3 of Scheme 1).

Table 3: Calculated Concentrations of Mg(II) Species in the Presence of 1 mM dATP and 1 mM EDTA[a]

$[Mg(II)]_{tot}$ (mM)	$[Mg(II)]_{free}$ (μM)	[MgdATP] (μM)	[MgEDTA] (μM)
0.030	0.10	1.3	28.7
0.070	0.25	3.1	66.8
0.20	0.81	9.8	190
0.40	2.0	25	373
0.70	5.8	67	627
0.90	11	122	767
1.2	31	270	899

[a] The concentration of Mg(II)dATP was estimated using MaxChelator program available at Web page http://www.stanford.edu/~cpatton/maxc.html.

When Figure 6A was repeated with dideoxy-terminated primers, no signal was observed (Figure 6C). This result suggests that the slow phase of fluorescence change is not caused by binding of the catalytic Mg(II) ion (step 3 or after of Scheme 1); instead, it occurs *after addition of Mg*(*II*) to the enzyme·DNA·MdNTP ternary complex (i.e., *after* step 3).

Confirmation of Results from Rh(III)dNTP without Using Analogues. While use of various analogues (e.g., dideoxy-terminated primers, dNTPαS, and different metal ions) has made it possible to dissect microscopic steps and characterize structures of intermediates, it is also likely that the analogues introduce unexpected perturbations. Thus, when the experimental properties of Pol β are shown to be different from those of other polymerases, or different from the computational results of the same polymerase, the use of analogues is often cited as the cause of the discrepancy. One way to address this issue is to perform different experiments by use of different analogues. If the results and interpretations from different experimental approaches are all consistent, then the likelihood of misinterpretation is minimized.

Furthermore, the information obtained from the use of analogues has led us to design new experiments without the use of any analogue. Taking into account that Pol β requires a relatively high concentration of Mg(II) for optimal activity, whereas it binds Mg(II)dNTP tightly ($K_{d,Mg}$ = 1.0 mM and $K_{d,MgdATP}$ = 46 μM (*1*)), it is possible to "dissect" two metal ions merely by limiting the amount of Mg(II) in the reaction buffer. As shown in Table 3, in a solution of 1 mM dATP, 1 mM EDTA, and 1.2 mM $MgCl_2$, the calculated concentra-

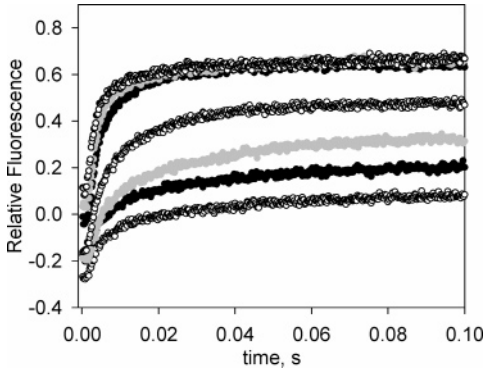

FIGURE 7: Stopped-flow 2-AP fluorescence assay of Mg(II)dATP binding to Pol β·DNA binary complex. For each reaction, one syringe contained Pol β with 19/36AP DNA substrate and 1 mM EDTA in assay buffer. The other syringe contained varying concentration of $MgCl_2$ with 2 mM dATP (final concentration after mixing is 1 mM) and 1 mM EDTA in assay buffer. The reactions were initiated by mixing 80 μL solutions from each syringe, and 2-aminopurine fluorescence was monitored during the reaction course. The final calculated concentrations of Mg(II)dATP are, according to Table 3 and from bottom to top, 1.3, 3.1, 9.8, 25, 67, 122, and 270 μM (note that the top three curves overlap).

tion of free Mg(II) is 31 μM, well below the $K_{d,Mg}$ and thus insufficient to support the catalysis, whereas that of Mg(II)-dATP is 270 μM, well above the $K_{d,MgdATP}$ and thus sufficient to saturate the Mg(II)dATP binding site. This prediction is well demonstrated by Figure 7, which shows results of stopped-flow 2-AP fluorescence assay at different calculated Mg(II)dATP concentrations. As can be seen, at these conditions, the binding of Mg(II)dATP induced the fast phase of fluorescence change only. These results resemble the data obtained with Cr(III)dTTP and Rh(III)dCTP, supporting the validity of using these metal ion complexes in our studies.

In order to reproduce results of single nucleotide incorporation from E·DNA·Rh(III)dNTP ternary complex with Mg(II), we utilized the sequential mixing mode of the stopped-flow instrument. Specifically, Pol β·DNA binary complex was premixed with Mg(II)dATP at conditions with a limiting amount of magnesium to form Pol β·DNA·Mg(II)dATP complex; then, after 150 ms of delay, the reaction was initiated by addition of excess Mg(II). In agreement with the Rh(III) results, the fast fluorescence transition was absent, presumably having occurred during the 150 ms delay before addition of excess Mg(II). Only the slow phase was observed, which fits well to a single exponential with $k = 1.09\ s^{-1}$ (Figure 8A). In a control experiment, when Pol β·DNA and dATP was premixed in the absence of magnesium for 150 ms, subsequent mixing with excess of Mg(II) resulted in biphasic fluorescence change (Figure 8B).

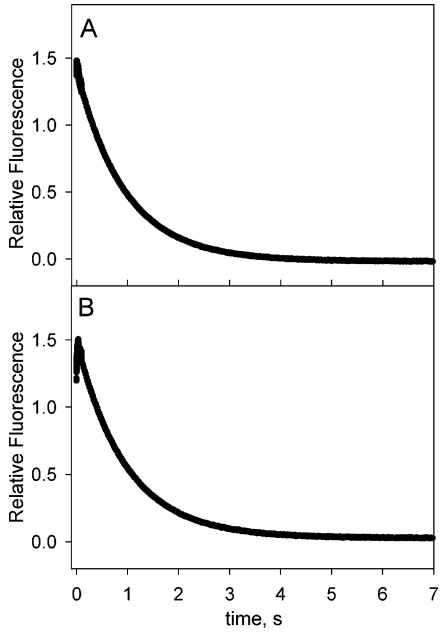

FIGURE 8: Three-syringe sequential mixing stopped-flow experiments for addition of catalytic Mg(II) to the E·DNA·Mg(II)dATP ternary complex. The reaction was designed to be analogous to Figure 6B but with Mg(II) instead of Rh(III). (A) One solution, containing Pol β, 19/36AP DNA substrate and 1 mM EDTA in the assay buffer, was first mixed with the second solution, containing 0.9 $MgCl_2$, 2 mM dATP and 1 mM EDTA in assay buffer. After a delay of 150 ms, the reaction was initiated by mixing with the third solution containing 22 mM $MgCl_2$ in assay buffer; and 2-aminopurine fluorescence was monitored during the reaction course. (B) Control experiment in which $MgCl_2$ was omitted from the second solution.

DISCUSSION

Updated Explanation of the Mechanism in Scheme 1. The results described in this paper provide new direct evidence supporting our previous interpretations that the fast fluorescence change observed in stopped-flow is due to the subdomain-closing conformational change observed in crystal structures (step 2 in Scheme 1), and that the rate of the slow phase reflects the rate-limiting chemical step (step 4 in Scheme 1). While the previous assignments were based primarily on the observations that the intermediate structure between the fast and the slow fluorescence transitions exists in the closed form, the present study provides evidence supporting that the fast phase reflects a major conformational change and that the rate of the slow phase reflects the rate of the chemical step. In addition, our stopped-flow data obtained under a variety of conditions clearly indicate that the slow fluorescence transition occurs after binding of the catalytic Mg(II) ion (i.e., after step 3 in Scheme 1).

For the fast fluorescence transition, our interpretation is based on the observation that it is differentially slowed by an increasing viscosity of the reaction buffer. In addition, it is further supported by its detection by both fluorophores. Since there is only one tryptophan residue in Pol β, located away from the active site, it can act as a reporter of conformational changes in Pol β, while 2-AP fluorescence reflects changes in the microenvironment of DNA conformations.

For the slow fluorescence transition, it is important to indicate that we do not suggest that it is caused by the chemical reaction, only that its rate is limited by chemistry, presumably because it occurs at a faster rate after the chemical step. Since the slow fluorescence change occurs in the opposite direction as the fast one with comparable amplitudes, and is observed for both tryptophan and 2-aminopurine fluorescence, it most likely reflects the reverse of the E to E′ step, i.e., E′ to E (step 6 in Scheme 1), the reopening of the closed form. This is our current working hypothesis. The chemical step (step 4) itself is unlikely to cause such fluorescence changes.

Further studies are necessary to measure the rates (and equilibrium constants) of the other steps in Scheme 1 (steps 1, 3, 5, 6, and 7). With such new information, we will be able to compare the rates of conformational change and chemistry under a variety of conditions including the incorporation of mismatched dNTP, dNTP analogues, and Pol β mutants, which will likely lead to unambiguous understanding of the mechanism of Pol β fidelity.

Our View on the Factors Contributing to the Fidelity of dNTP Incorporations. The mechanism of fidelity can be understood only by comparing the microscopic rates and structural intermediates for correct dNTP with those of mismatches. The kinetic scheme for correct dNTP incorporation, once completed, will serve to establish the framework for subsequent studies of misincorporations. While we are still at the early stage of such complete analyses, our present results provide further support that the chemical step, step 4, is the slowest step under single turnover experimental conditions monitored both by the dNTP incorporation in rapid quench experiments and by the fluorescence change in stopped-flow experiments. Since it is generally accepted that the chemical step is likely the slowest step in the incorporation of mismatched dNTP (*50*), the results presented here support our previous theory that the fidelity of Pol β is determined primarily by the chemical transition state (*3*), though differentiations between correct matches and mismatches can also occur at other steps.

Since our results for Pol β differ from the previously accepted concept that the subdomain-closing conformational change of DNA polymerases is the rate-limiting step and also the major fidelity-determining step (*2*), it has been suggested that Pol β is likely an exception among DNA polymerases. This issue can be addressed in the future by applying the three methods in this paper to other polymerases. In our view, it is not unlikely that different polymerases could have different rate-limiting steps for correct dNTP incorporation. The results of Pol β indicate that the chemical step is slower than the conformational change by less than a factor of 10 at pH 8.0 (though increasing to a factor of 100 at pH 7.0). The most important steps in understanding the mechanism of fidelity are to establish a complete and rigorous "kinetic and structural course of reaction" for correct base pairing, and then to use this platform to compare the mismatches with the correct base pairs.

Contradiction with Computational Results. Finally, we address the three recent reports on computational studies of the mechanism and reaction pathways of Pol β as mentioned in the introduction (*19*−*21*). Two of the key points in these studies are that "the binding of the catalytic Mg(II) and the rearrangement of Arg258 may be coupled and represent a slow step in Pol β's closing before chemistry", and that "Pol β subdomain closing requires presence of both nucleotide-binding and catalytic metal ions". Both points contradict our results since our data suggest that the subdomain-closing conformational change occurs *before* binding of the catalytic Mg(II) while the rate-limiting step occurs *after* binding of the catalytic Mg(II). While we acknowledge that all methodologies have limitations, our kinetic results have been self-consistent after applying additional, independent probes as described in this paper. Here we further discuss the differences between the computational results and our experimental results.

The suggestion that the rearrangement of Arg258 may be the rate-limiting step is not supported by our data, though it cannot be ruled out completely. While there is almost certainly some movement of side chains induced by binding of the catalytic metal ion, unless this results in a detectable intermediate species, it could not be considered to be a distinct step experimentally. Thus, even if binding of catalytic metal ion induces a slow isomerization, which is immediately followed by nucleotidyl transfer, this isomerization would not be kinetically distinct from nucleotidyl transfer and thus would have to be considered part of the chemical step. As shown in Scheme 1, we define the chemical step (step 4) as the step between the identifiable intermediate structure closest to the chemical transition state (Pol β·DNA·Mg(II)dNTP·Mg, which on the basis of crystal structures is essentially identical to Pol β·DNA·Cr(III)dNTP except for the orientation of some side chains of residues involved in the binding of the catalytic Mg(II)), and the identifiable intermediate structure immediately after the transition state (Pol β·DNA·Mg(II)PP_i·Mg(II), whose structure is not yet available but is likely to be nearly identical to the structure of Pol β·DNA·Cr(III)PCP) (*6*, *13*). Like any steps, the chemical step can be further dissected into multiple microscopic steps by use of different experimental or computational techniques at different time scales. It cannot be ruled out that reorientation of Arg258 is the slowest microscopic step within the chemical step, if the chemical step is further dissected. However, such a possibility remains to be demonstrated experimentally.

The second point of computational result, that binding of both Mg(II) ions are required for subdomain closing, contradicts our experimental data. The authors of the computational study rationalized the second point by suggesting that the difference results from the use of Cr(III) rather than Mg(II) (*21*), which we take to mean that our crystal structure of the intermediate, Pol β·DNA·Cr(III)dNTP ternary complex in the absence of the catalytic Mg(II) (*6*), exists in the closed form instead of the open form because Cr(III)dNTP instead of Mg(II)dNTP was used in the structure. If this were true, the stopped-flow result with Mg(II) should be very different. Since we showed that the stopped-flow results with Mg(II) can be dissected by use of different metal ions, and the results of the latter in turn led us to design experiments to dissect the stopped-flow results without using metal analogues, our results allow us to rule out the possibility that use of metal analogues causes the experimental result to be non-natural or erroneous.

Conclusion. We have performed further in-depth studies on the mechanism of Pol β, by use of new probes and analogues. The results provide new and additional evidence for the mechanism proposed in our previous studies, which differed from the mechanism suggested for other polymerases and was considered exceptional if believable by some critics. The results also allow us to address different mechanisms of Pol β concluded by the computational studies. Furthermore, the results set a good stage to study the mechanism of Pol β in further depth, and to study the mechanism of other DNA polymerases in a rigorous way.

SUPPORTING INFORMATION AVAILABLE

Experimental details of preparation and characterization of Rh(III)dCTP precomplex. This material is available free of charge via the Internet at http://pubs.acs.org.

REFERENCES

1. Dunlap, C. A., and Tsai, M.-D. (2002) Use of 2-Aminopurine and Tryptophan Fluorescence as Probes in Kinetic Analyses of DNA Polymerase β, *Biochemistry 41*, 11226−11235.
2. Kunkel, T. A., and Bebenek, K. (2000) DNA replication fidelity, *Annu. Rev. Biochem. 69*, 497−529.
3. Showalter, A. K., and Tsai, M.-D. (2002) A Reexamination of the Nucleotide Incorporation Fidelity of DNA Polymerases, *Biochemistry 41*, 10571−10576.
4. Kunkel, T. A. (2004) DNA Replication Fidelity, *J. Biol. Chem. 279*, 16895−16898.
5. Ahn, J., Werneburg, B. G., and Tsai, M.-D. (1997) DNA Polymerase β: Structure-Fidelity Relationship from Pre-Steady-State Kinetic Analyses of All Possible Correct and Incorrect Base Pairs for Wild-Type and R283A Mutant, *Biochemistry 36*, 1100−1107.
6. Arndt, J. W., Gong, W., Zhong, X., Showalter, A. K., Liu, J., Dunlap, C. A., Lin, Z., Paxson, C., Tsai, M.-D., and Chan, M. K. (2001) Insight into the Catalytic Mechanism of DNA Polymerase β: Structures of Intermediate Complexes, *Biochemistry 40*, 5368−5375.
7. Liu, J., and Tsai, M.-D. (2001) DNA Polymerase β: Pre-Steady-State Kinetic Analyses of dATPαS Stereoselectivity and Alteration of the Stereoselectivity by Various Metal Ions and by Site-Directed Mutagenesis, *Biochemistry 40*, 9014−9022.
8. Zhong, X., Patel, S. S., and Tsai, M.-D. (1998) DNA Polymerase β. 5. Dissecting the Functional Roles of the Two Metal Ions with Cr(III)dTTP, *J. Am. Chem. Soc. 120*, 235−236.
9. Zhong, X., Patel, S. S., Werneburg, B. G., and Tsai, M.-D. (1997) DNA polymerase β: Multiple conformational changes in the mechanism of catalysis, *Biochemistry 36*, 11891−11900.
10. Pelletier, H., Sawaya, M. R., Kumar, A., Wilson, S. H., and Kraut, J. (1994) Structures of ternary complexes of rat DNA polymerase β, a DNA template-primer, and ddCTP, *Science* (*Washington, D.C.*) *264*, 1891−903.
11. Pelletier, H., Sawaya, M. R., Wolfle, W., Wilson, S. H., and Kraut, J. (1996) Crystal structures of human DNA polymerase β complexed with DNA: Implications for catalytic mechanism, processivity, and fidelity, *Biochemistry 35*, 12742−12761.
12. Sawaya, M. R., Pelletier, H., Kumar, A., Wilson, S. H., and Kraut, J. (1994) Crystal structure of rat DNA polymerase β: evidence for a common polymerase mechanism, *Science* (*Washington, D.C.*) *264*, 1930−1935.
13. Sawaya, M. R., Prasad, R., Wilson, S. H., Kraut, J., and Pelletier, H. (1997) Crystal structures of human DNA polymerase β complexed with gapped and nicked DNA: Evidence for an induced fit mechanism, *Biochemistry 36*, 11205−11215.
14. Kim, S.-J., Beard, W. A., Harvey, J., Shock, D. D., Knutson, J. R., and Wilson, S. H. (2003) Rapid Segmental and Subdomain Motions of DNA Polymerase β, *J. Biol. Chem. 278*, 5072−5081.
15. Purohit, V., Grindley, N. D. F., and Joyce, C. M. (2003) Use of 2-Aminopurine Fluorescence To Examine Conformational Changes during Nucleotide Incorporation by DNA Polymerase I (Klenow Fragment), *Biochemistry 42*, 10200−10211.
16. Vande Berg, B. J., Beard, W. A., and Wilson, S. H. (2001) DNA structure and aspartate 276 influence nucleotide binding to human DNA polymerase β. Implication for the identity of the rate-limiting conformational change, *J. Biol. Chem. 276*, 3408−3416.
17. Fiala, K. A., and Suo, Z. (2004) Mechanism of DNA Polymerization Catalyzed by Sulfolobus solfataricus P2 DNA Polymerase IV, *Biochemistry 43*, 2116−2125.
18. Gohara, D. W., Arnold, J. J., and Cameron, C. E. (2004) Poliovirus RNA-Dependent RNA Polymerase (3Dpol): Kinetic, Thermodynamic, and Structural Analysis of Ribonucleotide Selection, *Biochemistry 43*, 5149−5158.
19. Radhakrishnan, R., and Schlick, T. (2004) Orchestration of cooperative events in DNA synthesis and repair mechanism unraveled by transition path sampling of DNA polymerase β's closing, *Proc. Natl. Acad. Sci. U.S.A. 101*, 5970−5975.
20. Yang, L., Beard, W. A., Wilson, S. H., Broyde, S., and Schlick, T. (2002) Polymerase β Simulations Suggest That Arg258 Rotation is a Slow Step Rather Than Large Subdomain Motions Per Se, *J. Mol. Biol. 317*, 651−671.
21. Yang, L., Arora, K., Beard, W. A., Wilson, S. H., and Schlick, T. (2004) Critical Role of Magnesium Ions in DNA Polymerase β's Closing and Active Site Assembly, *J. Am. Chem. Soc. 126*, 8441−8453.
22. Werneburg, B. G., Ahn, J., Zhong, X., Hondal, R. J., Kraynov, V. S., and Tsai, M.-D. (1996) DNA Polymerase β: Pre-Steady-State Kinetic Analysis and Roles of Arginine-283 in Catalysis and Fidelity, *Biochemistry 35*, 7041−7050.
23. Warshaw, M. M., and Cantor, C. R. (1970) Oligonucleotide interactions. IV. Conformational differences between deoxy- and ribodinucleoside phosphates, *Biopolymers 9*, 1079−103.
24. Lu, Z., Shorter, A. L., Lin, I., and Dunaway-Mariano, D. (1988) Preparation and configurational analysis of the stereoisomers of b,g-bidentate Rh(H2O)4ATP and a,b,g-tridentate Rh(H2O)3ATP. A new class of enzyme active site probes, *Inorg. Chem. 27*, 4135−4139.
25. Ayres, G. H., and Forrester, J. S. (1957) Preparation of rhodium-(III) perchlorate hexahydrate, *J. Inorg. Nucl. Chem. 3*, 365−366.
26. Cole, P. A., Burn, P., Takacs, B., and Walsh, C. T. (1994) Evaluation of the catalytic mechanism of recombinant human Csk (C-terminal Src kinase) using nucleotide analogs and viscosity effects, *J. Biol. Chem. 269*, 30880−30887.
27. Kanosue, Y., Kojima, S., and Ohkata, K. (2004) Influence of solvent viscosity on the rate of hydrolysis of dipeptides by carboxypeptidase Y, *J. Phys. Org. Chem. 17*, 448−457.
28. Kurz, L. C., Weitkamp, E., and Frieden, C. (1987) Adenosine deaminase: viscosity studies and the mechanism of binding of substrate and of ground- and transition-state analog inhibitors, *Biochemistry 26*, 3027−3032.
29. Lew, J., Taylor, S. S., and Adams, J. A. (1997) Identification of a partially rate-determining step in the catalytic mechanism of cAMP-dependent protein kinase: A transient kinetic study using stopped-flow fluorescence spectroscopy, *Biochemistry 36*, 6717−6724.
30. Shaffer, J., Sun, G., and Adams, J. A. (2001) Nucleotide Release and Associated Conformational Changes Regulate Function in the COOH-Terminal Src Kinase, Csk, *Biochemistry 40*, 11149−11155.
31. Gavish, B., and Werber, M. M. (1979) Viscosity-dependent structural fluctuations in enzyme catalysis, *Biochemistry 18*, 1269−1275.
32. Arnold, J. J., and Cameron, C. E. (2004) Poliovirus RNA-Dependent RNA Polymerase (3Dpol): Pre-Steady-State Kinetic Analysis of Ribonucleotide Incorporation in the Presence of Mg2+, *Biochemistry 43*, 5126−5137.
33. Einolf, H. J., and Guengerich, F. P. (2001) Fidelity of nucleotide insertion at 8-oxo-7,8-dihydroguanine by mammalian DNA polymerase d: steady-state and pre-steady-state kinetic analysis, *J. Biol. Chem. 276*, 3764−3771.
34. Kuchta, R. D., Benkovic, P., and Benkovic, S. J. (1988) Kinetic mechanism whereby DNA polymerase I (Klenow) replicates DNA with high fidelity, *Biochemistry 27*, 6716−6725.
35. Patel, S. S., Wong, I., and Johnson, K. A. (1991) Pre-steady-state kinetic analysis of processive DNA replication including complete characterization of an exonuclease-deficient mutant, *Biochemistry 30*, 511−525.
36. Washington, M. T., Prakash, L., and Prakash, S. (2001) Yeast DNA polymerase h utilizes an induced-fit mechanism of nucleotide incorporation, *Cell* (*Cambridge, Mass.*) *107*, 917−927.
37. Frey, M. W., Sowers, L. C., Millar, D. P., and Benkovic, S. J. (1995) The nucleotide analog 2-aminopurine as a spectroscopic probe of nucleotide incorporation by the Klenow fragment of Escherichia coli polymerase I and bacteriophage T4 DNA polymerase, *Biochemistry 34*, 9185−9192.
38. Joyce, C. M., and Steitz, T. A. (1994) Function and structure relationships in DNA polymerases, *Annu. Rev. Biochem. 63*, 777−822.
39. Steitz, T. A. (1999) DNA polymerases: structural diversity and common mechanisms, *J. Biol. Chem. 274*, 17395−17398.
40. Cowan, J. A. (1998) Metal Activation of Enzymes in Nucleic Acid Biochemistry, *Chem. Rev.* (*Washington, D.C.*) *98*, 1067−1087.
41. Cleland, W. W. (1982) Preparation of chromium(III) and cobalt-(III) nucleotides as chirality probes and inhibitors, *Methods Enzymol. 87*, 159−179.

42. Kuntzweiler, T. A., and Grisham, C. M. (1992) Inactivation and phosphorylation of sacroplasmic reticulum calcium-ATPase by magnesium. ATP analogs rhodium(III)-ATP and cobalt(III)-ATP, *Arch. Biochem. Biophys. 295*, 188−197.
43. Lu, Z., Shorter, A. L., and Dunaway-Mariano, D. (1993) Investigations of kinase substrate specificity with aqua rhodium(III) complexes of adenosine 5′-triphosphate, *Biochemistry 32*, 2378−2385.
44. Pappu, K. M., Kunnumal, B., and Serpersu, E. H. (1997) A new metal-binding site for yeast phosphoglycerate kinase as determined by the use of a metal-ATP analog, *Biophys. J. 72*, 928−935.
45. Serpersu, E. H., Bunk, S., and Schoner, W. (1990) How do magnesium-ATP analogs differentially modify high-affinity and low-affinity ATP binding sites of sodium−potassium ATPase?, *Eur. J. Biochem. 191*, 397−404.
46. Calvo, C. (1967) The crystal structure of a-magnesium pyrophosphate, *Acta Crystallogr. 23*, 289−295.
47. Shorter, A. L., Haromy, T. P., Scalzo-Brush, T., Knight, W. B., Dunaway-Mariano, D., and Sundaralingam, M. (1987) Structural and biochemical properties of bidentate tetraaquarhodium(III) complexes of inorganic pyrophosphate and adenosine 5′-diphosphate, *Biochemistry 26*, 2060−2066.
48. Sanders, C. R., II, Tian, G., and Tsai, M. D. (1989) Mechanism of adenylate kinase. Is there a relationship between local substrate dynamics, and local binding energy, and the catalytic mechanism?, *Biochemistry 28*, 9028−9043.
49. Torres, L. M., and Marzilli, L. G. (1991) Selective recognition and coordination by the [RhIII(tris(aminoethyl)amine)(H2O)2]3+ cation of the adenine nucleobase only when it is a constituent of a 5′-nucleotide, *J. Am. Chem. Soc. 113*, 4678−4679.
50. Johnson, K. A. (1993) Conformational coupling in DNA polymerase fidelity, *Annu. Rev. Biochem. 62*, 685−713.

BI047664W